Applied Mathematical Modelling 36 (2012) 4750–4759

Contents lists available at SciVerse ScienceDirect

Applied Mathematical Modelling

journal homepage: www.elsevier.com/locate/apm

Groundwater response to tidal fluctuation in a sloping leaky aquifer system

Mahdi Asadi-Aghbolaghi [a], Mo-Hsiung Chuang [b], Hund-Der Yeh [c,*]

[a] Water Engineering Department, Faculty of Agriculture, Shahrekord University, Shahrekord, Iran
[b] Department of Urban Planning and Disaster Management, Ming-Chuan University, Taoyuan, Taiwan
[c] Institute of Environmental Engineering, National Chiao Tung University, Hsinchu, Taiwan

ARTICLE INFO

Article history:
Received 30 January 2010
Received in revised form 5 December 2011
Accepted 12 December 2011
Available online 29 December 2011

Keywords:
Aquifer
Analytical solution
Leakage
Sloping aquifer
Tidal fluctuation
Mathematical modeling

ABSTRACT

The effect of tidal fluctuation on groundwater flow is an important issue from many aspects in coastal areas. This paper develops a new analytical solution to describe the groundwater fluctuation in a sloping coastal aquifer system which comprises an upper unconfined aquifer, a lower confined aquifer, and an aquitard in between. The solution is allowed to investigate the effects of bottom slope and leakage as well as aquifer parameters on head fluctuations in both unconfined and confined aquifers. The research result indicates that the effect of the bottom angle on the groundwater fluctuation and time lag is significant in the unconfined aquifer and not negligible if the leakage in the confined aquifer is large. In addition, the joint effects of aquifer parameters and bottom angle on groundwater fluctuation and time lag are also discussed.

© 2011 Elsevier Inc. All rights reserved.

1. Introduction

The investigation of tidal dynamics in coastal aquifers has been the subject of interest for many researchers since 1950s. Different methods have been adopted in an attempt to develop solutions for the problems using analytical approaches [1–15], numerical techniques [16–22], and experimental studies [20,23].

In many coastal aquifer systems, a leaky confined aquifer is overlain by an unconfined aquifer [24,25] and an aquitard is placed between them, where water seeps through the aquitard. Jiao and Tang [5] developed an analytical solution to investigate the influence of leakage on tidal response in a leaky confined aquifer with assuming that the hydraulic head is constant in the unconfined aquifer. Li et al. [9] presented an approximate analytical solution based on the linearized Boussinesq equation for unconfined aquifer to investigate the dynamic effect of phreatic aquifer on water fluctuation in confined aquifer. Li and Jiao [8] derived an analytical solution to examine the influence of leakage and storativity of the semi-permeable layer on groundwater-head change in a coastal confined aquifer. Jeng et al. [10] developed an analytical solution in a flat coupled coastal aquifer system. Their investigation showed that, under certain conditions, leakage from the confined aquifer can affect the water table fluctuation considerably in the phreatic aquifer. Ignoring these effects could lead to errors in estimating aquifer properties based on the tidal signals.

Recently, many researchers [26–32] have developed analytical solutions for flow in coastal aquifers with sloping beaches. For example, Teo et al. [11] developed a new higher-order solution for water table fluctuations in a coastal unconfined aquifer with a sloping beach. Chang et al. [31] derived the tide-induced groundwater fluctuations in an oceanic island with different slopes of beaches. Chen et al. [32] focused on the estimations of tidal characteristics and aquifer parameters for flow in a coastal aquifer with a sloping beach and bichromatic tidal system. Those analytical solutions have the advantages to

* Corresponding author. Tel.: +886 3 5731910; fax: +886 3 5725958.
E-mail address: hdyeh@mail.nctu.edu.tw (H.-D. Yeh).

0307-904X/$ - see front matter © 2011 Elsevier Inc. All rights reserved.
doi:10.1016/j.apm.2011.12.009

evaluate the parameter sensitivity in the mathematical model and identify the hydraulic parameters when coupling with an optimization approach in the data analysis.

Other researchers have focused on the coastal aquifer with a sloping impervious bed (e.g., [33,34]). Su et al. [33] developed Fourier series solutions to investigate the interaction between tidal waves and coastal unconfined aquifers overlaying a sloping impervious bed, using the linearized Boussinesq equation for the unconfined aquifer. Numerical analyses show that the Fourier series solutions capture two important features of the tidal waves; first, the tidal waves damp towards landward, and second, the half amplitude of the tide above the mean sea level is greater than that below it. Barlow and Reichard [34] gave a simplified conceptual model of saltwater leakage with a sloping coastal aquifer system and explained how to manage and prevent saltwater intrusion in the coastal regions of North America. Those articles indicate that the problems involved in sloping aquifer systems are important issues for groundwater flow in costal aquifers. To the best of our knowledge, an analytical solution for tide-induced fluctuations in a sloping aquifer system has never before been presented. The objective of this paper is to develop a new analytical solution for a sloping coastal aquifer system, comprising a leaky confined aquifer which is bounded from below by an impervious sloping bottom and separated from an overlying unconfined aquifer by an aquitard. The leakage through aquitard is driven by the difference in hydraulic head between the confined and unconfined aquifers. The linearized Boussinesq equation is considered to describe the groundwater flow of the unconfined aquifer. The joint effect of leakage and bottom angle is investigated and discussed in the paper. In addition, the joint effect of aquifer parameters and bottom angle on groundwater fluctuation and time lag is also addressed.

2. Mathematical model

2.1. Governing equation and boundary conditions

Fig. 1 shows a schematic diagram of a sloping coastal aquifer system with a vertical beach boundary, comprising a confined aquifer which is bounded from below by an impervious sloping bottom and separated from an overlying unconfined aquifer by an aquitard. Both confined and unconfined aquifers are isotropic and homogenous. In addition, there is a vertical leakage through the aquitard in the aquifer system. In this study, the effect of aquitard storage is assumed negligible; also, the flow in the unconfined aquifer is modeled by the linearized Boussinesq equation when the thickness of the unconfined aquifer is much greater than the tidal amplitude. These assumptions have been adopted by numerous researchers such as Jiao and Tang [5], Li and Jiao [7,8], Li et al. [9], Jeng et al. [10], Chuang and Yeh [13,15], and Li et al. [14]. The origin of x-axis is located at the intersection of the aquifer and beach face and the x-axis is horizontal and positive landward. Furthermore, the angle between the sloping bottom and x-axis is θ. The aquifers are infinite in y-direction and semi-infinite in x-direction. As such, the governing equations for the unconfined and confined aquifers can be described, respectively, as [10,33]:

$$S_1\frac{\partial h_1}{\partial t} = T_1\frac{\partial^2 h_1}{\partial x^2} + K_1\tan(\theta)\frac{\partial h_1}{\partial x} + L(h_2 - h_1) \tag{1}$$

and

$$S_2\frac{\partial h_2}{\partial t} = T_2\frac{\partial^2 h_2}{\partial x^2} + L(h_1 - h_2), \tag{2}$$

where h_1 and h_2 are the hydraulic heads for unconfined and confined aquifers, respectively; S_1 and S_2 are the storativities for unconfined and confined aquifers, respectively; T_1 and T_2 are the transmissivities for unconfined and confined aquifers, respectively, K_1 is the hydraulic conductivity for unconfined aquifer; and L is the leakage. The boundary conditions are specified as [10,13,15]

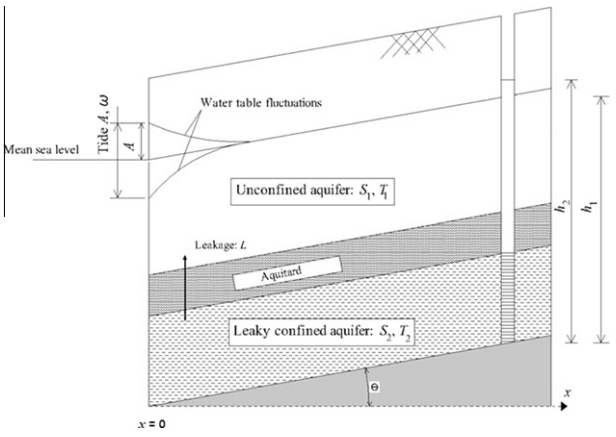

Fig. 1. Schematic diagram of a sloping coastal aquifer system, comprising an unconfined aquifer, an aquitard, and a confined aquifer.

$$h_1(0,t) = h_2(0,t) = h_{MSL} + Ae^{-i\omega t}, \tag{3a}$$

$$\left.\frac{\partial h_1(x,t)}{\partial x}\right|_{x\to\infty} = \left.\frac{\partial h_2(x,t)}{\partial x}\right|_{x\to\infty} = 0, \tag{3b}$$

where h_{MSL} is mean sea level, and A and ω are amplitude and frequency, respectively.

2.2. Development of the new analytical solution

From Eq. (1) h_1 can be expressed as

$$h_2 = h_1 + \frac{S_1}{L}\frac{\partial h_1}{\partial t} - \frac{T_1}{L}\frac{\partial^2 h_1}{\partial x^2} - \frac{K_1\tan(\theta)}{L}\frac{\partial h_1}{\partial x}. \tag{4}$$

Substituting h_1 in Eq. (4) into Eq. (2) obtains

$$\begin{aligned} &S_2\frac{\partial h_1}{\partial t} + \frac{S_1S_2}{L}\frac{\partial^2 h_1}{\partial t^2} - \frac{T_1S_2}{L}\frac{\partial^3 h_1}{\partial x^2\partial t} - \frac{K_1S_2\tan(\theta)}{L}\frac{\partial^2 h_1}{\partial x\partial t} - T_2\frac{\partial^2 h_1}{\partial x^2} - \frac{T_2S_1}{L}\frac{\partial^3 h_1}{\partial x^2\partial t} \\ &\quad + \frac{T_1T_2}{L}\frac{\partial^4 h_1}{\partial x^4} + \frac{K_1T_2\tan(\theta)}{L}\frac{\partial^3 h_1}{\partial x^3} + S_1\frac{\partial h_1}{\partial t} - T_1\frac{\partial^2 h_1}{\partial x^2} - K_1\tan(\theta)\frac{\partial h_1}{\partial x} = 0. \end{aligned} \tag{5}$$

To solve Eq. (5), because of the linearity of the model, only a single tide is used at the coastal boundary. The head fluctuations in both unconfined and confined aquifers are, respectively, expressed as [10,13–15]

$$h_1(x,t) = h_{MSL} + \mathrm{Re}[H_1(x)\exp(-i\omega t)], \tag{6a}$$

$$h_2(x,t) = h_{MSL} + \mathrm{Re}[H_2(x)\exp(-i\omega t)], \tag{6b}$$

where the absolute values of H_1 and H_2 represent the amplitudes of groundwater fluctuation for unconfined and confined aquifers, respectively. The boundary conditions, Eqs. (3a) and (3b), can then be rewritten as

$$H_1(0) = H_2(0) = A, \tag{6c}$$

$$\left.\frac{\partial H_1(x)}{\partial x}\right|_{x\to\infty} = \left.\frac{\partial H_2(x)}{\partial x}\right|_{x\to\infty} = 0. \tag{6d}$$

Substituting Eq. (6a) into Eq. (5) results in

$$\frac{d^4H_1}{dx^4} + a_1\frac{d^3H_1}{dx^3} + a_2\frac{d^2H_1}{dx^2} + a_3\frac{dH_1}{dx} + a_4H_1 = 0, \tag{7}$$

with

$$a_1 = \frac{K_1\tan(\theta)}{T_1}, \tag{8a}$$

$$a_2 = i\omega\left(\frac{S_2}{T_2} + \frac{S_1}{T_1}\right) - L\left(\frac{1}{T_1} + \frac{1}{T_2}\right), \tag{8b}$$

$$a_3 = \frac{K_1\tan(\theta)}{T_1T_2}(iS_2\omega - L), \tag{8c}$$

$$a_4 = -\frac{\omega}{T_1T_2}(iS_2L + iS_1L + S_1S_2\omega). \tag{8d}$$

The general solution for Eq. (7) can be expressed as [35]

$$H_1(x) = c_1e^{\lambda_1 x} + c_2e^{\lambda_2 x} + c_3e^{\lambda_3 x} + c_4e^{\lambda_4 x}, \tag{9}$$

where c_1, c_2, c_3, and c_4 are constant coefficients and can be determined using the boundary conditions. In addition, λ_1, λ_2, λ_3, and λ_4 are constants which can be written as

$$\lambda_1 = -\frac{a_1}{4} - \frac{1}{2}\sqrt{e_5 + e_6 + e_7} - \frac{1}{2}\sqrt{e_9 - e_6 - e_7 - e_8}, \tag{10a}$$

$$\lambda_2 = -\frac{a_1}{4} - \frac{1}{2}\sqrt{e_5 + e_6 + e_7} + \frac{1}{2}\sqrt{e_9 - e_6 - e_7 - e_8}, \tag{10b}$$

$$\lambda_3 = -\frac{a_1}{4} + \frac{1}{2}\sqrt{e_5 + e_6 + e_7} - \frac{1}{2}\sqrt{e_9 - e_6 - e_7 - e_8}, \tag{10c}$$

$$\lambda_4 = -\frac{a_1}{4} + \frac{1}{2}\sqrt{e_5 + e_6 + e_7} + \frac{1}{2}\sqrt{e_9 - e_6 - e_7 - e_8}, \tag{10d}$$

with

$$e_1 = 2^{\frac{1}{3}}(a_2^2 - 3a_1a_3 + 12a_4), \tag{11a}$$

$$e_2 = 2a_2^3 - 9a_1a_2a_3 + 27a_3^2 + 27a_1^2a_4 - 72a_2a_4, \tag{11b}$$

$$e_3 = \sqrt{-4(a_2^2 - 3a_1a_3 + 12a_4)^3 + (2a_2^3 - 9a_1a_2a_3 + 27a_3^2 + 27a_1^2a_4 - 27a_2a_4)^2}, \tag{11c}$$

$$e_4 = -a_1^3 + 4a_1a_2 - 8a_3, \tag{11d}$$

$$e_5 = \frac{a_1^2}{4} - \frac{2a_2}{3}, \tag{11e}$$

$$e_6 = \frac{e_1}{3(e_2 + e_3)^{\frac{1}{3}}}, \tag{11f}$$

$$e_7 = \frac{1}{3\sqrt[3]{2}}(e_2 + e_3)^{\frac{1}{3}}, \tag{11g}$$

$$e_8 = \frac{e_4}{4\sqrt{e_5 + e_6 + e_7}}, \tag{11h}$$

$$e_9 = \frac{a_1^2}{4} - \frac{4a_2}{3}. \tag{11i}$$

Since the hydraulic head at infinity should be bounded, the real part of λ_i should be negative and thus just two values out of four λ_i are considered. The final solution for H_1 can then be expressed as

$$H_1(x) = c_1 e^{\lambda_1 x} + c_3 e^{\lambda_3 x}. \tag{12}$$

Based on Eqs. (3a), (3b), and (9), the values of c_1 and c_3 can be determined as

$$c_1 = -A\frac{T_1\lambda_3^2 + iS_1\omega + K_1\lambda_3\tan(\theta)}{(\lambda_1 - \lambda_3)(T_1\lambda_1 + T_1\lambda_3 + K_1\tan(\theta))}, \tag{13a}$$

$$c_3 = -A\frac{T_1\lambda_1^2 + iS_1\omega + K_1\lambda_1\tan(\theta)}{(\lambda_1 - \lambda_3)(T_1\lambda_1 + T_1\lambda_3 + K_1\tan(\theta))}. \tag{13b}$$

The same procedure is also utilized to find $h_2(x,t)$. Eq. (2) can be expressed as

$$h_1 = h_2 + \frac{S_2}{L}\frac{\partial h_2}{\partial t} - \frac{T_2}{L}\frac{\partial^2 h_2}{\partial x^2}. \tag{14}$$

Substituting Eqs. (14) and (6b) into Eq. (1) yields

$$\frac{d^4H_2}{dx^4} + b_1\frac{d^3H_2}{dx^3} + b_2\frac{d^2H_2}{dx^2} + b_3\frac{dH_2}{dx} + b_4H_2 = 0, \tag{16}$$

where $b_1 = a_1$, $b_2 = a_2$, $b_3 = a_3$, and $b_4 = a_4$. The solution for $H_2(x)$ can therefore be expressed as

$$H_2(x) = c_5 e^{\lambda_5 x} + c_7 e^{\lambda_7 x},$$

with

$$c_5 = -A\frac{T_2\lambda_3^2 + iS_2\omega}{T_2(\lambda_1^2 - \lambda_3^2)}, \tag{17a}$$

$$c_7 = -A\frac{T_2\lambda_1^2 + iS_2\omega}{T_2(\lambda_1^2 - \lambda_3^2)}, \tag{17b}$$

where $\lambda_5 = \lambda_1$ and $\lambda_7 = \lambda_3$.

Note that the time lags Ω_1 and Ω_2 of groundwater response to tidal fluctuation can be calculated by $\arctan(\mathrm{Im}[H_1]/\mathrm{Re}[H_1])/\omega$ and $\arctan(\mathrm{Im}[H_2]/\mathrm{Re}[H_2])/\omega$ for unconfined and confined aquifers, respectively [7].

2.3. Special case

If both confined and unconfined aquifers are flat, i.e., $\theta = 0$, the constants a_1, a_3, b_1, and b_3 will be all zero. Eqs. (7) and (14) will, respectively, reduce to

$$\frac{d^4H_1}{dx^4} + \left(i\omega\left(\frac{S_2}{T_2}+\frac{S_1}{T_1}\right) - L\left(\frac{1}{T_1}+\frac{1}{T_2}\right)\right)\frac{d^2H_1}{dx^2} + -\frac{\omega}{T_1T_2}(iS_2L + iS_1L + S_1S_2\omega)H_1 = 0 \tag{18}$$

and

$$\frac{d^4H_2}{dx^4} + \left(i\omega\left(\frac{S_2}{T_2}+\frac{S_1}{T_1}\right) - L\left(\frac{1}{T_1}+\frac{1}{T_2}\right)\right)\frac{d^2H_2}{dx^2} + -\frac{\omega}{T_1T_2}(iS_2L + iS_1L + S_1S_2\omega)H_2 = 0, \tag{19}$$

which are exactly the same as those in Jeng et al. [10], Eqs. (8) and (16). It is worth noting that in both the present solution and Jeng et al.'s [10] solution, the method of separation of variables was utilized to find analytical solutions for the problems.

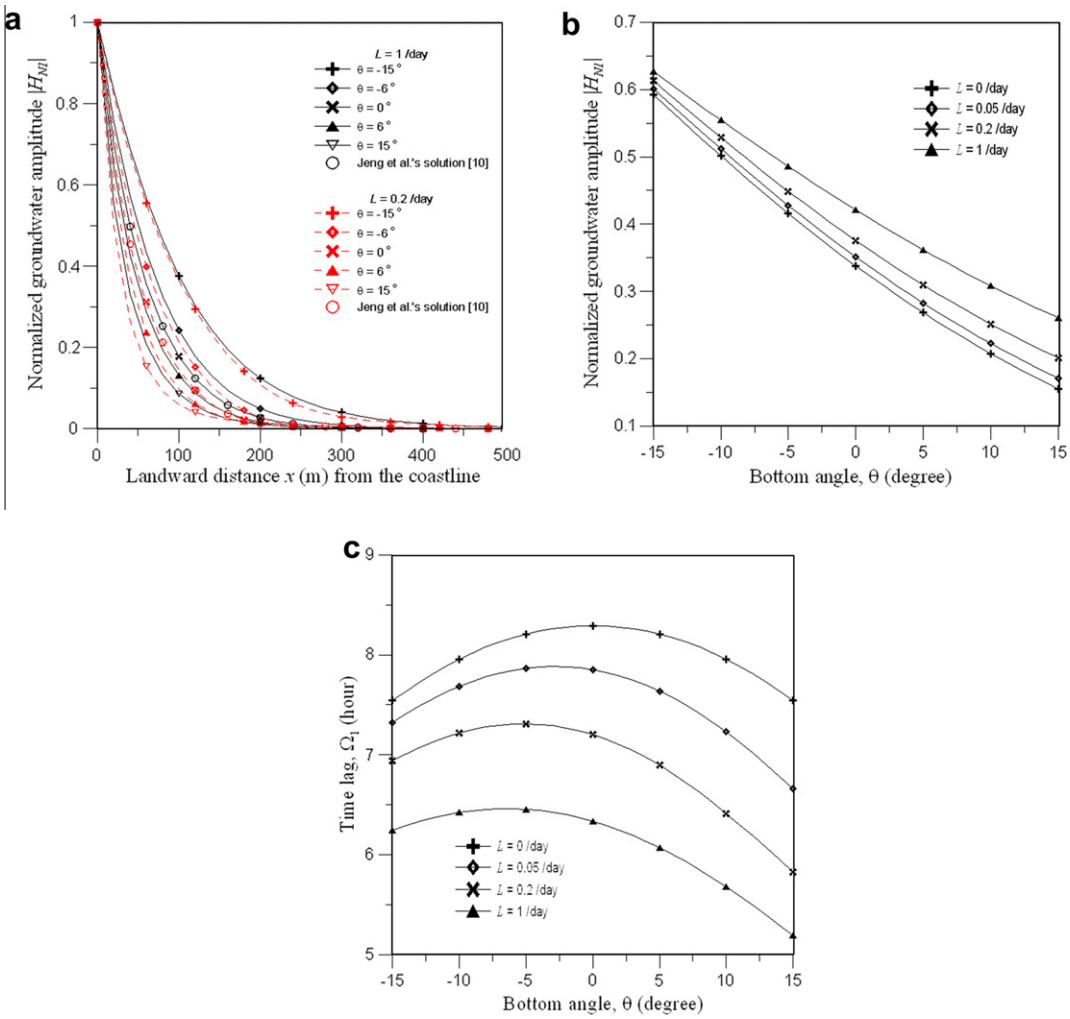

Fig. 2. The curves of (a) H_{N1} versus x for $L = 0.2$/day and $L = 1$/day when the bottom angle $\theta = -15°$, 0°, and 15°, (b) H_{N1} versus θ at $x = 50$ m, and (c) Ω_1 versus θ at $x = 100$ m in unconfined aquifer.

3. Results and discussion

In this section several numerical examples are introduced to investigate the effects of leakage, bottom slope, and aquifer parameters on the head fluctuations in both unconfined and confined aquifers. As mentioned above that the aquifer system in Jeng et al.'s solution [10] can be considered as a special case of the present solution. The values of parameters and physical data adopted from their paper for the examples are $L = 0.2$/day or $L = 1$/day, $T_1 = T_2 = 2000\ m^2$/day, $S_1 = 0.3$, $S_2 = 0.001$, $A = 0.65$ m, $\omega = 2\pi$ rad/day, $h_{MSL} = 0$, and $K_1 = 200$ m/day.

Two normalized aquifer parameters, $T = T_1/T_2$ and $S = S_1/S_2$, used in Jeng et al. [10] are also adopted in this paper. The subscript N in the normalized parameters $H_{N1} = H_1/A$ and $H_{N2} = H_2/A$ denotes a normalized form. Furthermore, joint effects of leakage, bottom angle, and aquifer parameters on the time lag are discussed in this section.

3.1. Joint effects of leakage and bottom angle

Fig. 2a shows the curves of normalized amplitude of groundwater fluctuation in the unconfined aquifer (i.e., H_{N1}) versus landward distance x for $L = 0.2$/day and $L = 1$/day with the bottom slope $\theta = -15°$, 0, and 15°. As indicated in the figure, the curve predicted by the Jeng et al.'s solution [10] is identical to the one when $\theta = 0°$. The figure shows that H_{N1} decreases with both θ and x for $L = 0.2$/day and 1/day. The figure also indicates that the intrusion distance is about 500 m when $\theta = -15°$ and smaller than 300 m when $\theta > 0°$. Fig. 2b shows the curves of H_{N1} versus θ at $x = 50$ m for $L = 0$, 0.05, 0.2, and 1/day. This figure demonstrates that H_{N1} decreases with increasing θ for all L and, however, increases with L. Those results indicate that the prediction of H_{N1} will lead to large errors without considering the bottom angle. Fig. 2c illustrates the curves of time lag

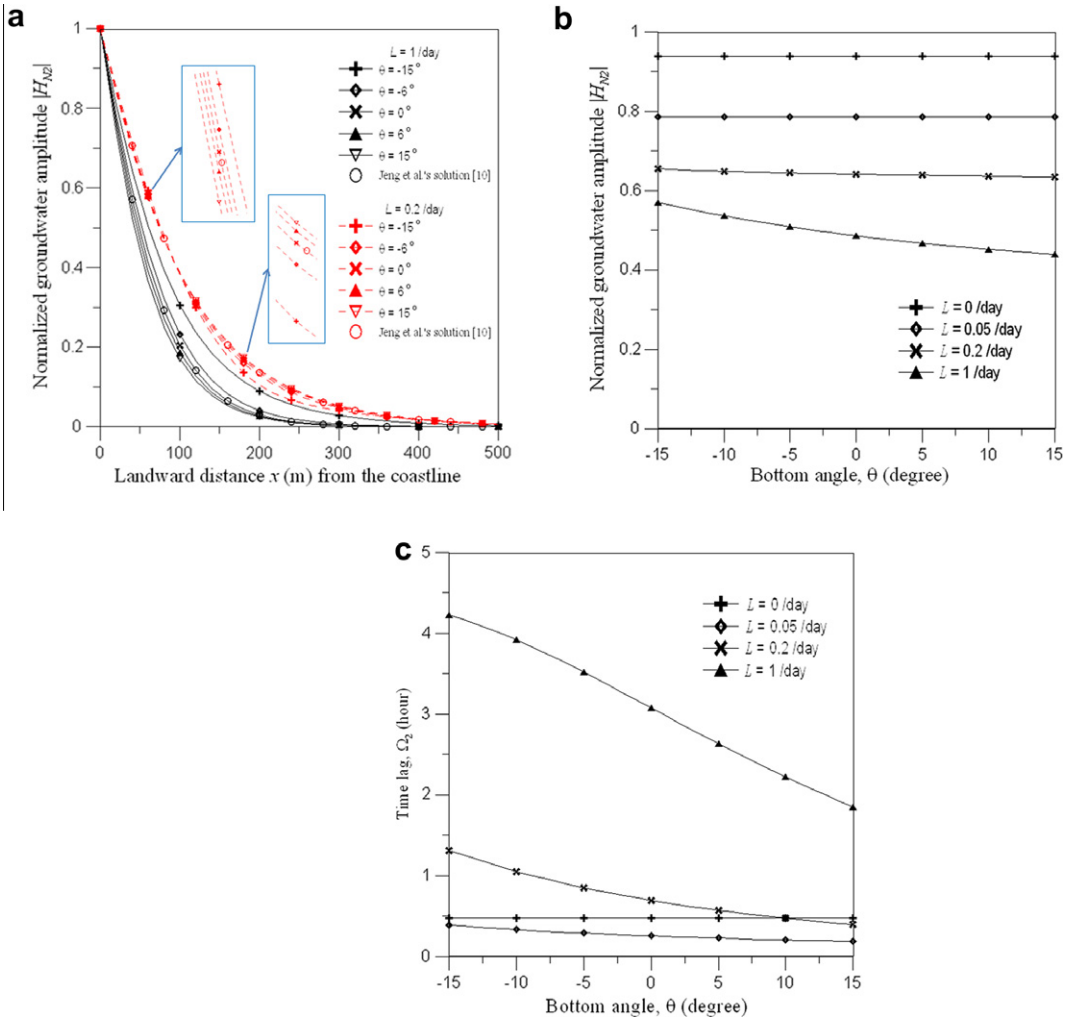

Fig. 3. The curves of (a) H_{N2} versus x for $L = 0.2$/day and $L = 1$/day when $\theta = -15°$, 0°, and 15°, (b) H_{N2} versus θ at $x = 50$ m, and (c) Ω_2 versus θ at $x = 100$ m in confined aquifer.

Ω_1 versus θ at $x = 100$ m. This figure shows Ω_1 increases with θ, reaches to its maximum value, and then decreases with increasing θ. Specifically, the time lag reaches its peak value at $\theta = 0°$ when $L = 0$/day and at $\theta = -5°$ when $L = 1$/day. Fig. 2c also shows that Ω_1 decreases with increasing L.

Fig. 3a shows the curves of normalized amplitude of groundwater fluctuation in confined aquifer (H_{N2}) versus x for $L = 0.2$/day and 1/day and $\theta = -15°$, 0°, and 15°. The hollow circles stands for Jeng et al.'s solution [10] which exactly matches with the curve of the present solution when $\theta = 0°$ as shown in the figure, indicating that Jeng et al.'s solution [10] can be considered as a special case of the present solution. Furthermore, this figure shows that the H_{N2} increases as θ decreases when $L = 1$/day, and the largest difference in H_{N2} between $\theta = -15°$ and 15° is 0.1428 occurring at $x = 80$ m. The curves for the case of $L = 0.2$/day exhibit that H_{N2} decreases as θ increases when $x < 100$ m but increases with θ when $x > 100$ m. Fig. 3b shows the curves of H_{N2} versus θ at $x = 50$ m, indicating that H_{N2} is independent of θ when $L < 0.2$/day. However, H_{N2} decreases with increasing θ when $L = 1$/day. Obviously, the effect of θ on H_{N2} should be taken into account in the tidal sloping aquifer system if the aquitard leakage is large. Fig. 3c shows Ω_2 versus θ at $x = 100$ m for $L = 0$, 0.05, 0.2, and 1/day. This figure shows that Ω_2 decreases as θ increases when the leakage is not negligible, however, Ω_2 is independent of θ for the case that $L = 0$. Also the figure indicates that the effect of leakage on Ω_2 in confined aquifers decreases with increasing θ.

3.2. Joint effects of aquifer parameters and bottom angle

In this section the joint effects of θ and normalized aquifer parameters (i.e., T and S) on the groundwater fluctuation in a leaky sloping aquifer system are investigated. When the leakage is large the effect of θ on H_{N2} is noticeable; therefore, the leakage is assumed to be $L = 1$/day in the following analyses. Fig. 4a shows the curves of H_{N1} versus T at $x = 50$ m and for θ

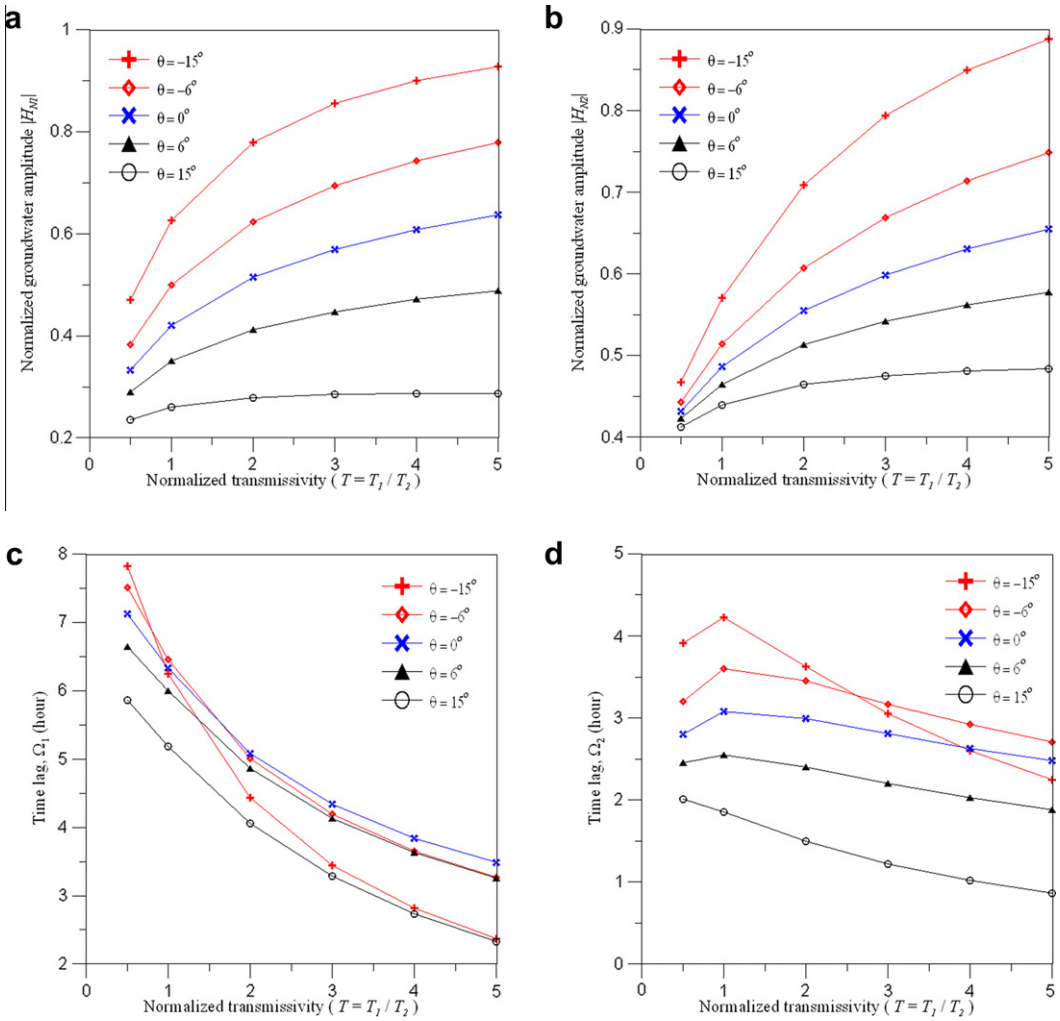

Fig. 4. The curves of normalized amplitude of groundwater fluctuation versus T at $x = 50$ m in (a) unconfined aquifer and (b) confined aquifer and the curves of time lag versus T at $x = 100$ m in (c) unconfined aquifer and (d) confined aquifer.

value from -15° to 15°, and those of H_{N2} versus T are in Fig. 4b. These two figures exhibit that both H_{N1} and H_{N2} increases with T for all values of θ. They also show the effect of bottom angle on the normalized groundwater amplitude in the unconfined and confined aquifers increases with T. These results indicate that the joint effect of T and θ on the normalized groundwater amplitude is very significant when T is large. Fig. 4c and d show the curves of time lag versus T for unconfined and confined aquifers, respectively, at $x = 100$ m. The behavior of Ω_1 in response to the change in T in unconfined aquifers is shown in Fig. 4c. The curves show that Ω_1 decreases with increasing T, and, its decreasing rate increases as θ decreases. Since at $T = 0.5$, Ω_1 increases as θ decreases, therefore, the curve intersect each other. The curves of Ω_2 versus T are depicted in Fig. 4d for different values of θ, which are different from those in unconfined ones. The figure shows that Ω_2 decreases with increasing T for $\theta = 15^\circ$. However, for other values of θ, the curves exhibit that Ω_2 has a peak value near $T = 1$ and then decreases when the value of T departs from one. In addition, the curve of $\theta = -15^\circ$ has the largest decreasing rate.

The curves of H_{N1} versus S are shown in Fig. 5a and those of H_{N2} versus S are in Fig. 5b at $x = 50$ m for θ from -15° to 15°. These two figures show a similar trend for both H_{N1} and H_{N2}, i.e. H_{N1} and H_{N2} decrease with increasing S and θ. In addition, the curves demonstrate that the effect of θ on H_{N1} and H_{N2} decreases with increasing S. The difference between the values of H_{N1} for $\theta = -15^\circ$ and 15° is 0.5040 when $S = 50$, and 0.3661 when $S = 300$. On the other hand, the difference between the values of H_{N2} for $\theta = -15^\circ$ and 15° is 0.3430 when $S = 50$, and 0.1315 when $S = 300$. These results indicate that the effect of θ on H_{N1} is larger than that of H_{N2}. Fig. 5c and d show the time lag versus S at $x = 100$ m in unconfined and confined aquifers, respectively. Fig. 5c displays that time lag in the unconfined aquifer, Ω_1, increases with S for all values of θ. The curves for the case that $\theta \geqslant 0$ show that Ω_1 decreases with increasing θ for all values of S. On the other hand, for the case that $\theta < 0$, the increasing rate of Ω_1 with respect to S increases as θ decreases. The figure also shows the time lag for the cases of $\theta = 6^\circ$ and -6° as well as the cases of $\theta = 15^\circ$ and -15° are very close when $S < 75$. However, since the increasing rate

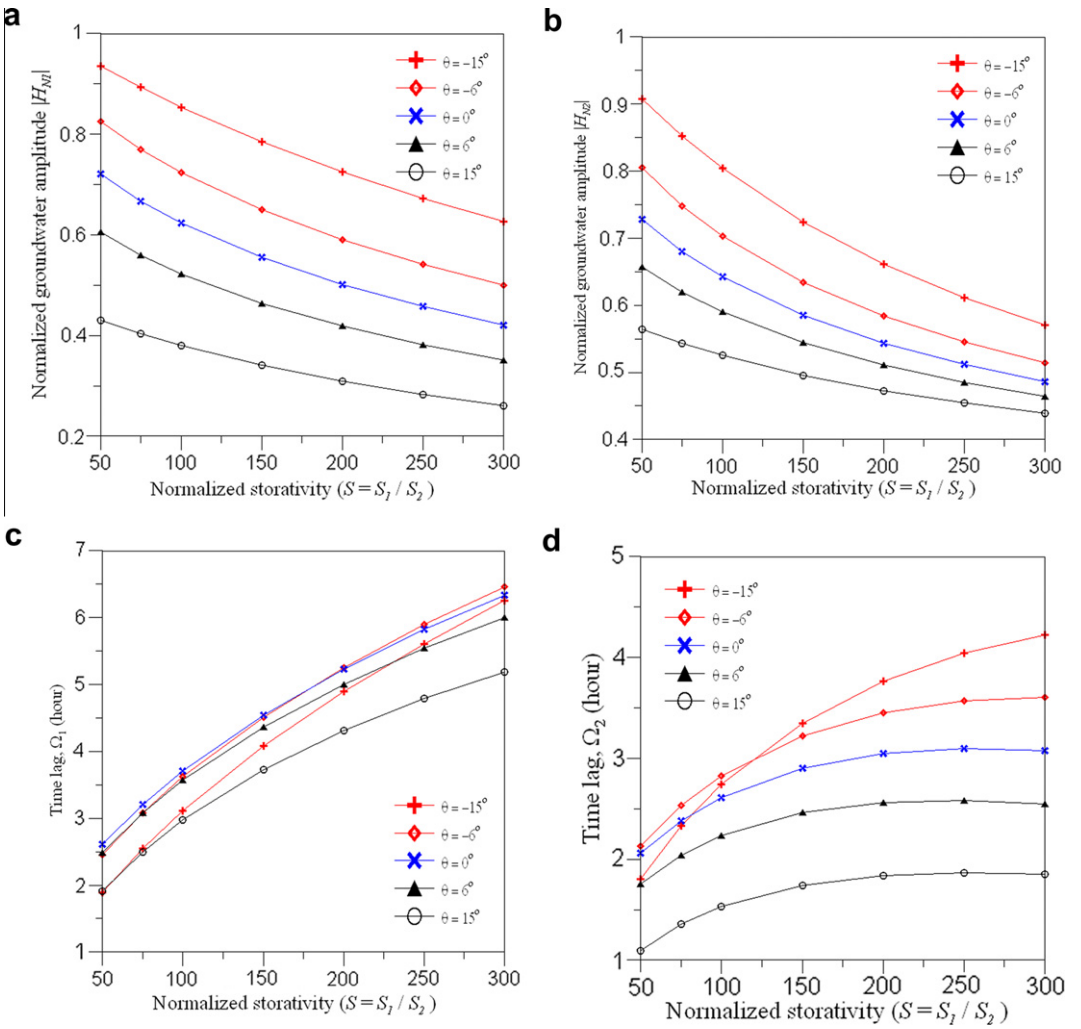

Fig. 5. The curves of normalized amplitude of groundwater fluctuation versus S at $x = 50$ m in (a) unconfined aquifer and (b) confined aquifer, and the curves of time lag of groundwater fluctuation versus S at $x = 100$ m in (c) unconfined aquifer and (d) confined aquifer.

is larger for negative slopes than for the positive one, the differences of the time lag increase with S. Fig. 5d demonstrates that Ω_2 increases with S for all θ's. It is interesting to point out that Ω_2 decreases with increasing θ when $S \geqslant 150$. However, Ω_2 increases with θ for θ from -15° to -6°, and decreases with increasing θ when $\theta > -6^\circ$ and $S \leqslant 100$.

4. Concluding remarks

An analytical solution has been developed to investigate head fluctuation in a sloping coastal aquifer system, comprising an unconfined aquifer, an aquitard, and a confined aquifer. The results predicted from this newly developed solution show that bottom angle (θ) has a significant effect on tide-induced groundwater fluctuation. The groundwater amplitude decreases with increasing θ for all leakage (L) values in the unconfined aquifer, and the effect of the bottom angle on the groundwater fluctuation cannot be ignored if the leakage in the confined aquifer is large. The results also show that the time lag reaches the peak value when θ falls in the range between -5° and 0° in the unconfined aquifer, and decreases with increasing θ in the confined aquifer when $L > 0$. It is found that for all values of θ normalized amplitude increases with normalized transmissivity (T) but decreases with increasing normalized storativity (S) in both unconfined and confined aquifers. The time lag decreases with increasing T in unconfined aquifer for a wide range of θ. However, the time lag in confined aquifer decreases with increasing T only for the case $\theta = 15^\circ$ and has a maximum value near $T = 1$ for other values of θ. On the other hand, the time lag increases with S for all θ in the confined and unconfined aquifers.

Acknowledgements

This study was partly supported by the Taiwan National Science Council under the grants NSC 99-2221-E-009-062-MY3, NSC 100-2221-E-009-106, and NSC100-3113-E-007-011. The authors would like to thank two anonymous reviewers for their valuable and constructive comments that help improve the clarity of our presentation.

References

[1] A.E. Taigbenu, A.L. James, H.D.C. Alexander, Boundary integral solution to seawater intrusion into coastal aquifers, Water Resour. Res. 20 (8) (1984) 1150–1158.
[2] P. Nielsen, Tidal dynamics of the water table in beaches, Water Resour. Res. 26 (9) (1990) 2127–2134.
[3] D.O. Gregg, An analysis of groundwater fluctuations caused by ocean tides in Glynn County, Georgia, Ground Water 4 (3) (1966) 24–32.
[4] H. Sun, A two-dimensional analytical solution of groundwater response to tidal loading in an estuary, Water Resour. Res. 33 (6) (1997) 1429–1435.
[5] J.J. Jiao, Z. Tang, An analytical solution of groundwater response to tidal fluctuation in a leaky confined aquifer, Water Resour. Res. 35 (3) (1999) 747–751.
[6] L. Li, D.A. Barry, F. Stagnitti, J.Y. Parlange, D.S. Jeng, Beach water table fluctuations due to spring-neap tides: moving boundary effects, Adv. Water Resour. 23 (8) (2000) 817–824.
[7] H. Li, J.J. Jiao, Tide-induced groundwater fluctuation in a coastal leaky confined aquifer system extending under the sea, Water Resour. Res. 37 (5) (2001) 1165–1171.
[8] H. Li, J.J. Jiao, Analytical studies of groundwater-head fluctuation in a coastal confined aquifer overlain by a leaky layer with storage, Adv. Water Resour. 24 (5) (2001) 565–573.
[9] L. Li, D.A. Barry, D.S. Jeng, Tidal fluctuations in a leaky confined aquifer: dynamic effects of an overlying phreatic aquifer, Water Resour. Res. 37 (4) (2001) 1095–1098.
[10] D.S. Jeng, L. Li, D.A. Barry, Analytical solution for tidal propagation in a coupled semi-confined/phreatic coastal aquifer, Adv. Water Resour. 25 (5) (2002) 577–584.
[11] H.T. Teo, D.S. Jeng, B.R. Seymour, D.A. Barry, L. Li, A new analytical solution for water table fluctuations in coastal aquifers with sloping beaches, Adv. Water Resour. 26 (12) (2003) 1239–1247.
[12] D.S. Jeng, X. Mao, P. Enot, D.A. Barry, L. Li, Spring-neap tide-induced beach water table fluctuations in a sloping coastal aquifer, Water Resour. Res. 41 (7) (2005) W07026.
[13] M.H. Chuang, H.D. Yeh, An analytical solution for the head distribution in a tidal leaky aquifer extending an infinite distance under the sea, Adv. Water Resour. 30 (3) (2007) 439–445.
[14] H.L. Li, G. Li, J. Cheng, M.C. Boufadely, Tide-induced head fluctuations in a confined aquifer with sediment covering its outlet at the sea floor, Water Resour. Res. 43 (2007), doi:10.1029/2005WR004724.
[15] M.H. Chuang, H.D. Yeh, Analytical solution for tidal propagation in a leaky aquifer extending finite distance under the sea, J. Hydraul. Eng., ASCE 134 (4) (2008) 447–454.
[16] R.E. Volker, Predicting the movement of seawater into a coastal aquifer, Tech. Pap. 51, Aust. Water Resour. Counc., Dept. of Natl. Devel. Energy, Aust. Gov. Publ., 1980.
[17] C.S. Fang, S.N. Wang, W. Harrison, Groundwater flow in a sandy tidal beach: two dimensional finite element analysis, Water Resour. Res. 8 (1) (1972) 121–128.
[18] L. Li, D.A. Barry, C.B. Pattiarachi, Numerical modelling of tide induced beach water table fluctuations, Coastal Eng. 30 (1997) 105–123.
[19] A.J. Baird, T. Mason, D.P. Horn, Validation of a Boussinesq model of beach ground water behaviour, Mar. Geol. 148 (1998) 55–69.
[20] B. Ataie-Ashtiani, R.E. Volker, D.A. Lockington, Numerical and experimental study of seepage in unconfined aquifers with a periodic boundary condition, J. Hydrol. 222 (1999) 165–184.
[21] H.L. Li, J.J. Jiao, Numerical studies of tide-induced groundwater level change in a multi-layered coastal leaky aquifer system, in: XIV International Conference on Computational Methods in Water Resources, Delft, The Netherlands, 2002.
[22] S. Liu, H. Li, M.C. Boufadel, G. Li, Numerical simulation of the effect of the sloping submarine outlet-capping on tidal groundwater head fluctuation in confined coastal aquifers, J. Hydrol. 361 (2008) 339–348.
[23] N. Cartwright, P. Nielsen, L. Liy, Experimental observations of water table waves in an unconfined aquifer with a sloping boundary, Adv. Water Resour. 27 (10) (2004) 991–1004.
[24] J.K. White, T.O.L. Roberts, The significance of groundwater tidal fluctuations, in: W.B. Wilkinson (Ed.), Groundwater Problems in Urban Areas: Proceeding of the International Conference Organized by the Institution of Civil Engineers and Held in London, 2–3 June 1993, Thomas Telford, London, 1994, pp. 31–42.

[25] C.X. Chen, J. Jiao, Numerical simulation of pumping tests in multilayer wells with non-Darcian flow in the wellbore, Ground Water 37 (3) (1999) 465–474.
[26] J.Y. Parlange, F. Stagnitti, J.L. Starr, R.D. Braddock, Free-surface flow in porous media and periodic solution of the shallow-flow approximation, J. Hydrol. 70 (1984) 251–263.
[27] Z. Song, L. Li, J. Kong, H. Zhang, A new analytical solution of tidal water table fluctuations in a coastal unconfined aquifer, J. Hydrol. 340 (2007) 256–260.
[28] J. Kong, Z.Y. Song, P. Xin, C.J. Shen, A new analytical solution for tide-induced groundwater fluctuations in an unconfined aquifer with a sloping beach, China Ocean Eng. 25 (3) (2011) 479–494.
[29] M.E. Roberts, M.G. Trefry, N. Fowkes, A.P. Bassom, P.C. Abbott, Water-table response to tidal forcing at sloping beaches, J. Eng. Math. 69 (4) (2010) 291–311.
[30] R.K. Bansal, S.K. Das, Response of an unconfined sloping aquifer to constant recharge and seepage from the stream of varying water level, Water Resour. Manage. 25 (3) (2011) 893–911.
[31] Y.C. Chang, D.S. Jeng, H.D. Yeh, Tidal propagation in an oceanic island with sloping beaches, Hydrol. Earth Syst. Sci. 14 (7) (2010) 1341–1351.
[32] Y.J. Chen, G.Y. Chen, H.D. Yeh, D.S. Jeng, Estimations of tidal characteristics and aquifer parameters via tide-induced head changes in coastal observation wells, Hydrol. Earth Syst. Sci. 15 (5) (2011) 1473–1482.
[33] N. Su, F. Liu, V. Anh, Tides as phase-modulated waves inducing periodic groundwater flow in coastal aquifers overlaying a sloping impervious base, Environ. Model. Software 18 (2003) 937–942.
[34] P.M. Barlow, E.G. Reichard, Saltwater intrusion in coastal regions of North America, Hydrogeology J. 18 (1) (2010) 247–260.
[35] E. Kreyszig, Advanced Engineering Mathematics, eighth ed., John Wiley and Sons, Singapore, 1999. p. 132.